NF-κB constitutes a potential therapeutic target in high-risk myelodysplastic syndrome

Thorsten Braun, Gabrielle Carvalho, Arnaud Coquelle, Marie-Catherine Vozenin, Pascale Lepelley, François Hirsch, Jean-Jacques Kiladjian, Vincent Ribrag, Pierre Fenaux, and Guido Kroemer

Myelodysplastic syndrome (MDS) is a preneoplastic condition that frequently develops into overt acute myeloid leukemia (AML). The P39 MDS/AML cell line manifested constitutive NF-κB activation. In this cell line, NF-κB inhibition by small interfering RNAs specific for p65 or chemical inhibitors including bortezomib resulted in the down-regulation of apoptosis-inhibitory NF-κB target genes and subsequent cell death accompanied by loss of mitochondrial transmembrane potential as well as by the mitochondrial release of the caspase activator cytochrome *c* and the caspase-independent death effectors endonuclease G and apoptosis-inducing factor (AIF). Bone marrow cells from high-risk MDS patients also exhibited constitutive NF-κB activation similar to bone marrow samples from MDS/AML patients. Purified hematopoietic stem cells ($CD34^+$) and immature myeloid cells ($CD33^+$) from high-risk MDS patients demonstrated the nuclear translocation of the p65 NF-κB subunit. The frequency of cells with nuclear p65 correlated with blast counts, apoptosis suppression, and disease progression. NF-κB activation was confined to those cells that carried MDS-associated cytogenetic alterations. Since NF-κB inhibition induced rapid apoptosis of bone marrow cells from high-risk MDS patients, we postulate that NF-κB activation is responsible for the progressive suppression of apoptosis affecting differentiating MDS cells and thus contributes to malignant transformation. NF-κB inhibition may constitute a novel therapeutic strategy if apoptosis induction of MDS stem cells is the goal. (Blood. 2006;107:1156-1165)

Introduction

Myelodysplastic syndrome (MDS) is a group of hematopoietic stem cell disorders characterized by ineffective hematopoiesis leading to blood cytopenias and by a high risk of progression to acute myeloid leukemia (AML).[1] MDS is classified based on morphology and blast cell percentage in blood and bone marrow (French American British [FAB] classification and World Health Organization [WHO] classification).[2] The main prognostic factors of MDS, for progression to AML and survival, include the number and severity of cytopenias, the percentage of marrow blasts, and bone marrow cytogenetic abnormalities. Those factors are combined in an International Prognostic Scoring System (IPSS)[3] that distinguishes 4 subgroups with significantly different risk of progression to AML and survival: low, intermediate 1 (int 1), intermediate 2 (int 2), and high.

Activating mutations of oncogenes and inactivating mutations of tumor suppressor genes have been identified in a number of genes in MDS and AML, although none of them identified mutations specific for MDS.[4] This includes activating mutations of the RAS pathway[5] as well as frequent methylation silencing of the *CDKN2B* (*p15INK4B*) gene,[6] whereas *TP53* (*p53*) mutations are less common.[7]

MDS can be viewed as a preleukemic condition in which apoptosis aborts the differentiation products of potentially malignant mutated stem cells.[8,9] Low-risk MDS (with low or int 1 IPSS scores) is characterized by increased intramedullary apoptosis of progenitors, leading to inefficient hematopoiesis and cytopenia. On the contrary, in high-risk MDS (with int 2 or high IPSS scores) progressive increase in marrow blasts with reduced apoptotic capacities is seen, and blastic infiltration leads to cytopenias through marrow failure.[10] The death of MDS cells exhibits common characteristics of apoptosis including mitochondrial membrane permeabilization (MMP)[11]; caspase activation[12]; plasma membrane phosphatidylserine exposure[13]; and activation of death receptors such as CD95,[14,15] TNF-R,[16] or TRAIL receptors.[17] Previous studies suggested that the expression of proapoptotic proteins (Bak, Bad, Bcl-X_S) has a positive

From the Centre National de la Recherche Scientifique, Unite Mixté de Recherche (UMR) 8125, Institut Gustave Roussy, Villejuif, France; Unité propre de la recherche et de l'enseignement superieur (UPRES EA) 2710, Institut Gustave Roussy, Villejuif, France; Laboratoire d'Hématologie, Hôpital Calmette, Lille, France; Institut National de la Santé et de la Recherche Médicale (INSERM) U542, Paris XI University, Hôpital Paul Brousse, Villejuif, France; Service d'Hématologie Clinique, Hôpital Avicenne, Assistance Publique–Hôpitaux de Paris (AP-HP), Université Paris 13, Bobigny, France; and Service d'Hématologie Clinique, Institut Gustave Roussy, Villejuif, France.

Submitted May 18, 2005; accepted September 25, 2005. Prepublished online as *Blood* First Edition Paper, October 13, 2005; DOI 10.1182/blood-2005-05-1989.

G.K. is supported by Cancéropôle Ile-de-France, Ligue Nationale contre le Cancer, Fondation de France, Association pour la Recherche sur le Cancer, and European Community (Active p53, TransDeath). T.B. is supported by a fellowship from the Etablissement Français du Sang. G.C. is supported by the Association NRB Vaincre le Cancer.

T.B., G.C., A.C., and M.-C.V. performed the experiments and analyzed the data; P.L., J.-J.K., V.R., and P.F. provided bone marrow samples and essential clinical information on patients; F.H. and P.F. participated in the conception of the study; and G.K. conceived and directed the study.

T.B. and G.C. contributed equally to this paper.

Reprints: Guido Kroemer, CNRS-UMR8125, Institut Gustave Roussy, PR1, 38 rue Camille Desmoulins, F-94805 Villejuif, France; e-mail: kroemer@igr.fr.

The publication costs of this article were defrayed in part by page charge payment. Therefore, and solely to indicate this fact, this article is hereby marked "advertisement" in accordance with 18 U.S.C. section 1734.

prognostic value in MDS, whereas the expression of antiapoptotic proteins (Bcl-2, Bcl-X_L) has a negative prognostic value,[18] suggesting that loss of the apoptotic program could favor the MDS-to-AML transition.

The NF-κB family of transcription factors can potently suppress apoptosis.[19] Constitutive activation of NF-κB was reported for various solid tumors and hematologic malignancies.[20,21] In multiple myeloma, NF-κB activity leads to expression of the antiapoptotic protein Bcl-X_L leading to chemoresistance.[22] Aberrant expression of NF-κB family proteins has been described for other B- and T-cell neoplasias, including in those induced by oncogenic viruses, namely Epstein Barr virus (EBV) and HTLV-1, both of which encode NF-κB activators.[23,24] Finally, NF-κB is found to be activated in primitive AML cells leading to expression of antiapoptotic c-IAP2[25] through mechanisms that are not entirely elucidated.

Classically, the members of the NF-κB family form dimers (classically heterodimers of p65 with p50), which under nonstimulated conditions are retained in the cytoplasm through interactions with inhibitory molecules of the inhibitor of NF-κB (IκB) family.[26] Following activation by a number of stimuli that include cytokines, various stress signals, and bacterial and viral products, the IκB molecules get phosphorylated by IκB kinases (IKKs) and degraded by the ubiquitin-proteasome pathway.[27] This liberates the NF-κB dimers that are free to translocate to the nucleus and activate their target genes.[28] Inhibitors of NF-κB activation, notably inhibitors of IKKs, are being designed and are undergoing preclinical evaluation.[29] Moreover, an indirect NF-κB and proteasome inhibitor, bortezomib (Velcade), has been approved for the treatment of multiple myeloma[30] and is under clinical evaluation for the treatment of other hematologic malignancies.[31]

The goal of the present study was to determine NF-κB activation in MDS, since the current literature[32-34] provides no consensus on the correlation between NF-κB activation and disease progression. Here we show that constitutive NF-κB activation is a property of MDS blasts, that NF-κB activation is restricted to the population of MDS bone marrow cells that carry MDS-associated cytogenetic alterations (and hence is likewise a cell-autonomous phenomenon), that the degree of NF-κB activation correlates with high-risk MDS, and that inhibition of NF-κB can precipitate apoptosis both in MDS cell lines and in bone marrow blasts from high-risk MDS patients.

Patients, materials, and methods

Patients

A total of 57 MDS patients and 7 healthy subjects were included in our study (Table 1). Informed consent of all patients and healthy subjects was provided according to the Declaration of Helsinki. Approval for this study was obtained from the Institut Gustave Roussy institutional review board. MDS patients were previously untreated except for supportive care. The diagnosis of MDS was based on peripheral blood counts and cytology of peripheral blood and bone marrow (BM) according to the WHO classification[2] and conventional cytogenetic analysis. These data permitted the evaluation of the individual IPSS score for each patient.[3] BM aspirates were obtained, after informed consent, into syringes containing media supplemented with EDTA. The BM mononuclear cell (BMMNC) fraction was isolated by density gradient centrifugation using Ficoll-Paque PLUS (Amersham Biosciences, Sunnyvale, CA).

Table 1. Characteristics of MDS patients

Patient no.	Karyotype	BM blasts, %	Cytopenia	IPSS	WHO classification
1	46, XY	1	1	0	RA
2	46, XX	1	1	0	RA
3	46, XY	2	1	0	RA
4	46, XY	2	2	0.5	RCMD
5	46, XY	3	3	0.5	RCMD
6	46, XY	4	1	0	RA
7	46, XX	5	3	1	RAEB-1
8	46, XY	6	2	1	RAEB-1
9	46, XY	7	3	1	RAEB-1
10	46, XY	8	2	1	RAEB-1
11	46, XY	9	3	1	RAEB-1
12	46, XY	11	2	2	RAEB-2
13	46, XY	11	2	2	RAEB-2
14	46, XY	11	2	2	RAEB-2
15	46, XX	12	2	2	RAEB-2
16	46, XY	15	2	2	RAEB-2
17	46, XY	16	2	2	RAEB-2
18	46, XY	19	1	1.5	RAEB-2
19	46, XY	19	2	2	RAEB-2
20	46, XY	19	3	2	RAEB-2
21	46, XX	27	2	NA	MDS/AML
22	47, XY, +8	0	2	1	RCMD
23	47, XY, +8	2	1	0.5	RA
24	47, XX, +8	2	2	1	RCMD
25	47, XY, +8	2	2	1	RA
26	47, XY, +8	4	0	0.5	RA
27	47, XX, +8	7	1	1	RAEB-1
28	47, XX, +8	7	2	1.5	RAEB-1
29	47, XY, +8	9	1	1	RAEB-1
30	47, XY, +8	9	1	1	RAEB-1
31	47, XX, +8	15	1	2	RAEB-2
32	47, XX, +8	38	2	NA	MDS/AML
33	47, XX, +8	49	2	NA	MDS/AML
34	46, XY, del(5q)	1	2	0.5	5q syndrome
35	46, XX, del(5q)	2	1	0	5q syndrome
36	46, XX, del(5q)	4	1	0	5q syndrome
37	46, XX, del(5q)	4	1	0	5q syndrome
38	46, XX, del(5q)	4	2	0.5	5q syndrome
39	46, XX, del(5q)	5	1	0.5	RAEB-1
40	46, XY, del(5q)	9	3	1	RAEB-1
41	46, XX, del(5q)	32	3	NA	MDS/AML
42	46, XX, del(5q)	71	2	NA	MDS/AML
43	46, XX, del(20q)	2	3	0.5	RCMD
44	46, XY, del(20q)	4	1	0	RA
45	46, XX, del(20q)	5	3	1	RAEB-1
46	46, XY, del(20q)	6	3	1	RAEB-1
47	46, XX, del(20q)	7	2	1	RAEB-1
48	45, XY, −Y	4	1	0	RA
49	45, XY, −19	42	2	NA	MDS/AML
50	45, XY, −7	2	1	1	RA
51	45, XX, −7	3	2	1.5	RCMD
52	45, XY, −7	8	0	1.5	RAEB-1
53	45, XY, −7	14	3	3	RAEB-2
54	45, XX, −7	19	2	3	RAEB-2
55	45, XX, −7	48	1	NA	MDS/AML
56	Complex	17	2	3	RAEB-2
57	Complex	19	3	3	RAEB-2

RA indicates refractory anemia; RCMD, refractory cytopenia with multilineage dysplasia; RAEB, refractory anemia with excess of blasts (5%-9% BM blasts RAEB-1, 10%-19% BM blasts RAEB-2); NA, not applicable; and 5q syndrome, MDS associated with isolated del(5q).

Cells and culture conditions

The high-risk MDS cell line P39/Tsugane (kindly provided by Dr Yoshida Takeda, Japan) was cultured in RPMI 1640 (Gibco, Carlsbad, CA) supplemented with 10% heat-inactivated fetal calf serum, 2 mM L-glutamine, 100 IU/mL penicillin, and 100 g/mL streptomycin as described.[35]

BM cells and cord blood (CB) cells were isolated and processed as follows: after density gradient separation $CD34^+$ and $CD33^+$ cells were isolated from the BMMNC compartment by positive selection with the

MiniMacs system (Miltenyi Biotec, Bergisch Gladbach, Germany) following manufacturer's instructions. Cells were maintained in Iscove modified Dulbecco medium (IMDM; Gibco) supplemented with 10% heat-inactivated fetal calf serum.

Knock-down of p65 by small interfering RNA (siRNA)

Cells were transfected with the Nucleofactor system (Amaxa, Cologne, Germany) using siRNAs specific for emerin[36] or using scramble and p65 (Upstate, Lake Placid, NY) for sequenced p65 (duplex of 5′-rgrCrCrCUrAUrCrCrCUUUrArCrgUrCrA TT-3′/5′-UrgrArCrgUrArArArgrgrgrAUrArgrgr grC TT-3′).

Assessment of apoptosis

P39 or patient cells (10^5) were resuspended in 1 mL of culture medium and incubated in the presence or absence of 5 μM BAY11-7082 (Sigma, St Louis, MO), 2.5 nM bortezomib, 100 μM z-VAD-fmk, 1 μM all-*trans* retinoic acid (ATRA; Sigma), or 0.25 μM vitamin D_3 (Calbiochem, San Diego, CA) for 24 hours. Apoptotic cells were detected by flow cytometry analysis using a FACScan (Becton Dickinson, Mountain View, CA) as described previously.[37,38] Cells were stained with propidium iodide (PI; 5 μg/mL; Sigma) for 15 minutes and concomitantly with 40 nM fluorochrome $DiOC_6(3)$ (3,3′ dihexyloxacarbocyanine iodide; Molecular Probes, Eugene, OR) for 15 minutes at 37°C, or with annexin-V–FITC (Becton Dickinson) following manufacturer's instructions for 15 minutes at 4°C for determination of the mitochondrial transmembrane potential ($\Delta\psi_m$) and phosphatidyl serine exposure.[39,40]

Immunoblots

Lysates from 5×10^6 cells, with or without exposure to BAY11-7082 (Biomol, Plymouth Meeting, PA) or bortezomib (OrthoBiotec, Bridgewater, NJ) for 24 hours in addition with z-VAD-fmk (100 μM), were separated on sodium dodecyl sulfate (SDS)–polyacrylamide gel and electroblotted onto PVDF membranes. For mitochondrial protein release, cells were pelleted after treatment, washed, and incubated with buffer containing 0.05% digitonin on ice for 5 minutes. Polyclonal rabbit antibodies (Abs) were used to recognize the 14.5-kDa subunit of the active caspase-3 (Cell Signaling Technology, Beverly, MA). Bcl-X_L (mouse monoclonal Ab; Chemicon, Temecula, CA), IκB-P (mouse monoclonal Ab; Cell Signaling Technology) and c-IAP2 (rabbit polyclonal Ab; Santa Cruz Biotechnology, Santa Cruz, CA), g-tubulin (mouse monoclonal Ab; Sigma-Aldrich, St Louis, MO), actin (mouse monoclonal Ab; Chemicon), or glyceraldehydes-3-phosphate dehydrogenase (GAPDH; mouse monoclonal Ab; Chemicon) were also used. Blots were stained with either goat anti–rabbit peroxidase-labeled or goat anti–mouse peroxidase-labeled secondary Ab (Amersham, Arlington Heights, IL) and were revealed using an enhanced chemiluminescence (ECL) detection system (Amersham).

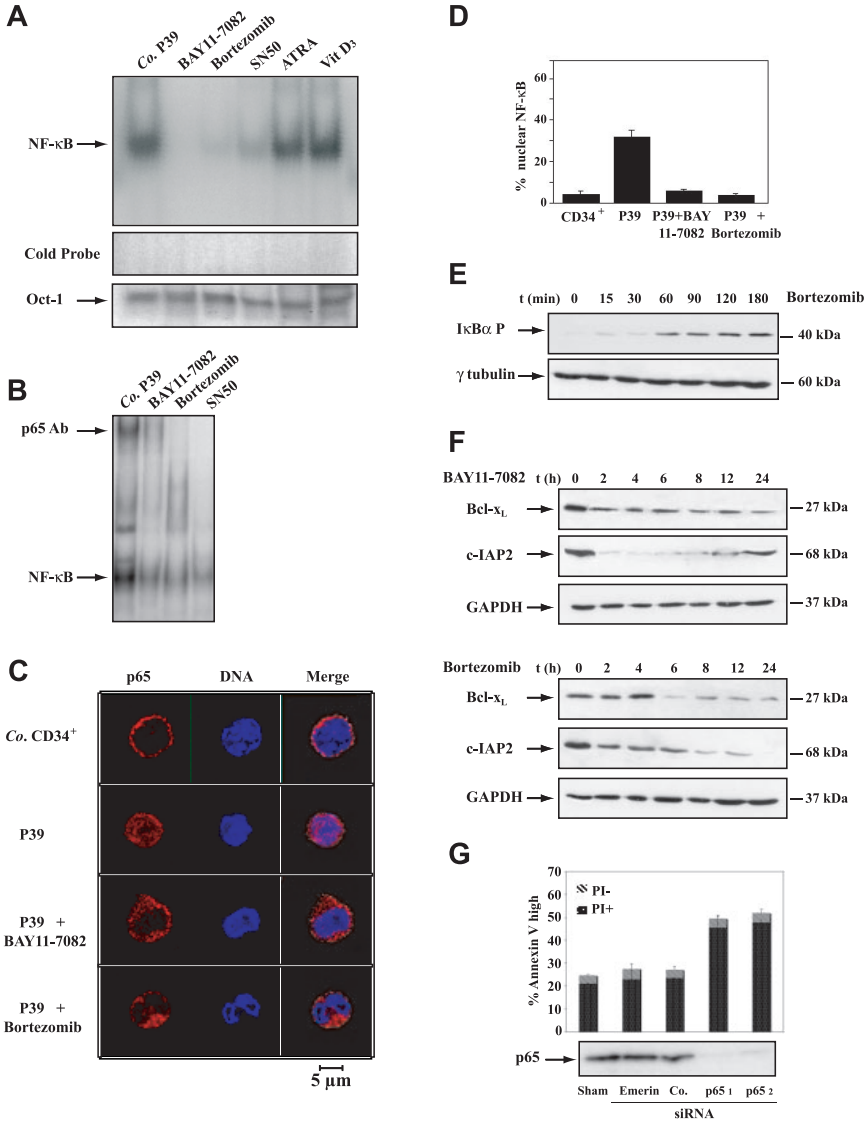

Figure 1. Signs of NF-κB activity in P39 cells. (A) NF-κB activation determined by EMSA staining. P39 cells were left untreated (control, Co) or cultured in the presence of BAY11-7082 (5 μM, 6 h), bortezomib (2.5 nM, 6 h), SN50 (36 μM, 6 h), ATRA (1 μM, 48 h), or vitamin D_3 (Vit D_3; 0.25 μM, 48 h), followed by the generation of nuclear extracts and EMSA assays. The transcription factor Oct-1 was monitored to assure equal loading. (B) Detection of p65 by supershift in nuclear extracts of P39 cells. NF-κB was detected by EMSA as in panel A with the difference that a p65-specific antibody was added to the extracts, leading to the apparition of a specific supershifted band. (C) Detection of p65 by confocal immunofluorescence microscopy. Cells treated as in panel A were immobilized on coverslips, fixed, permeabilized, and subjected to immunostaining of p65 (red fluorescence) and nuclear counterstaining (blue), as detailed in "Patients, materials, and methods." Images were visualized under an LSM 510 confocal microscope equipped with a 63 ×/1.32-0.6 oil-immersion objective lens (Zeiss, Oberkochen, Germany) and a CCD camera (Zeiss). (D) Quantification of immunofluorescence data obtained in panel B. Values are means (X±SD, n = 3). (E) Bortezomib effect on IκB. P39 cells were treated for the indicated period with bortezomib (2.5 nM), followed by immunoblot detection of phosphorylated IκB. (F) Effects of bortezomib and BAY11-7082 on NF-κB target genes. After exposure of cells to either of the 2 NF-κB inhibitors, cell extracts were prepared and the abundance of Bcl-X_L and c-IAP2 was determined. All experiments were repeated at least 3 times, yielding similar results. (G) Lethal knock-down of p65. P39 cells were sham-transfected or transfected with siRNAs that affect the expression of emerin or p65. Immunoblots were performed 72 hours after transfection (bottom panel) and the frequency of annexin-V^+ cells was monitored by cytofluorometry. Values are means (X±SD, n = 3).

Nuclear protein extraction and electrophoretic mobility shift assay (EMSA)

Nuclear extracts were obtained from the P39 cell line, BMMNCs, and $CD34^+$ and $CD33^+$ cells. P39 cells were cultured for 6 hours in the presence or absence of 5 μM BAY 11-7082 or 2.5 nM bortezomib, 36 μM SN50 (Biomol), 1 μM ATRA (Sigma), and 0.25 μM vitamin D_3 (Calbiochem), and nuclear extracts were prepared in lysis buffer (20 mM HEPES [pH 7.9], 350 mM NaCl, 1 mM EGTA, 1 mM dithiothreitol) and complete protease inhibitors (Roche, Indianapolis, IN) as described previously.[41] Extracts were then mixed with binding buffer (25 mM Tris Hcl [pH 8], 50 mM KCl, 6.25 mM $MgCl_2$, 0.5 mM EDTA, 0.5 mM dithiothreitol, 10% glycerol, and poly[dI-dC] 1 μg/μL) and the γ-^{32}P–labeled NF-κB oligonucleotide probe (5′-ACAAGGGACTTTCCGCTGGGGACTTTCCAG-3′; Invitrogen, Carlsbad, CA) together with a T4 polynucleotide kinase (Roche) and incubated for 30 minutes at room temperature. Specificity was assessed by incubating nuclear extracts of treated cells with the nonradiolabeled NF-κB probe or mutated NF-κB probe (5′-ACAACTCACTTTCCGCTGCTCACTTTCCAG-3′; Invitrogen). In addition, we used a γ-^{32}P–labeled oligonucleotide probe specific for Oct-1 (Invitrogen) to determine equal loading of nuclear extracts, and we performed supershifts of NF-κB with a p65-specific antibody (Santa Cruz Biotechnology) using standard protocols.[41]

Immunofluorescence

In separate experiments, 10^5 P39 or patient cells were allowed to adhere on polylysine-L coverslips (Sigma) and were fixed in 4% paraformaldehyde at room temperature. Cells were then permeabilized with either Triton X-100 0.05% (Boehringer Mannheim, Mannheim, Germany) or SDS 0.1% for 10 minutes, washed in PBS, and stained with p65 (rabbit polyclonal Ab; Santa Cruz Biotechnology), cytochrome *c* (mouse monoclonal Ab; BD Pharmingen, Heidelberg, Germany), endonuclease G (rabbit polyclonal Ab; Pro-Science, Woburn, MA), apoptosis-inducing factor (AIF; rabbit polyclonal Ab; Chemicon), or anti-Hsp60 (mouse monoclonal Ab or rabbit polyclonal Ab; Sigma and Stressgen, San Diego, CA; respectively) and revealed either with a goat anti–rabbit and goat anti–mouse IgG coupled with Alexa 568 (red) or Alexa 488 (green) fluorochromes (Molecular Probes) or a goat anti–rabbit and goat anti–mouse IgG conjugated with a streptavidin/peroxidase complex (DAKO, Carpinteria, CA), after inhibition of endogenous peroxidases with 10% H_2O_2. DNA of cells was counterstained with either TO-PRO3 (Molecular Probes) or Hoechst 33324 (Molecular Probes), allowing the discernment of chromatin condensation. Two hundred cells for each slide were examined independently with a LSM 510 confocal microscope (Zeiss, Thornwood, NY) at × 63 magnification. Background correction of fluorescence was performed with the LSM 5 image browser (Zeiss).

IκB measurement

Lysates obtained from 3×10^6 cells with or without prior exposure to 2.5 nM bortezomib were separated on 12% SDS–polyacrylamide gel and electroblotted onto nitrocellulose membranes. Blots were first stained with phospho-IκBα (mouse monoclonal Ab; Cell Signaling Technology) and revealed with antimouse peroxidase-labeled secondary Abs (Amersham). Revelation was performed using an ECL detection system (Amersham).

FISH

Ex vivo BMMNCs were allowed to adhere on polylysine-L glass slides (Sigma) and were fixed in methanol–acetic acid (3:1) for 30 minutes or stained for nuclear p65 revealed by streptavidin/peroxidase after inhibition of endogenous peroxidases with 10% H_2O_2. Interphase fluorescence in situ hybridization (FISH) was performed following manufacturer's instructions by using a rhodamine and fluorescein–labeled dual probe (D7Z1/D8Z1) for simultaneous detection of the chromosome 7 and 8 centromere (Qbiogene, Irvine, CA). DNA of nuclei was counterstained with DAPI II (Vectashield,

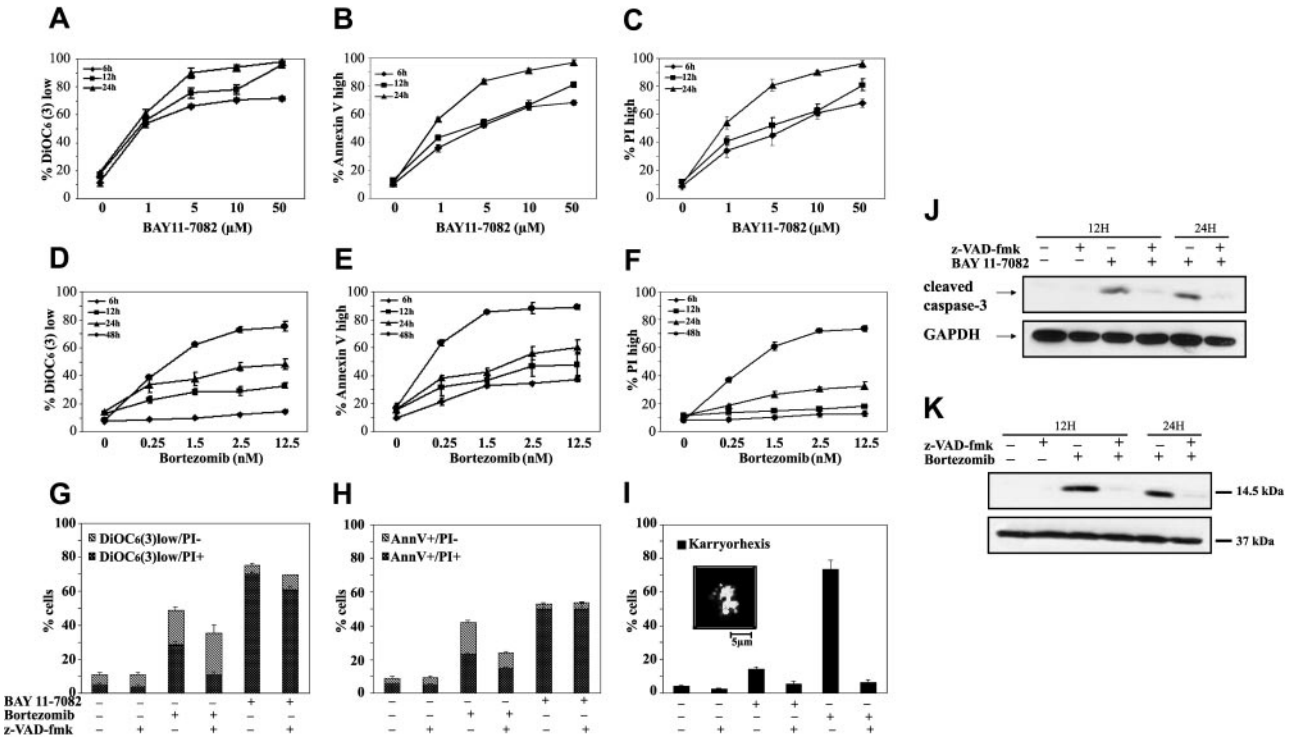

Figure 2. Induction of apoptosis by NF-κB inhibition in P39 cells. (A-F) Kinetics of apoptosis induction by different doses of BAY11-7082 (A-C) and bortezomib (D-F). P39 cells were cultured in the presence of either of 2 NF-κB inhibitors for the indicated period and then stained with $DiOC_6(3)$ (A,D), FITC-labeled annexin-V (B,E), and/or PI (C,F) to determine the frequency of $\Delta\psi_m^{low}$, phosphatidylserine$^+$, and dead (PI^+) cells, respectively. (G-I) Effect of z-VAD-fmk on apoptotic characteristics of P39 cells dying upon NF-κB inhibition. P39 cells were cultured for 24 hours in the absence or presence of BAY11-7082 (5 μM), bortezomib (2.5 nM), or z-VAD-fmk (100 μM), followed by staining with $DiOC_6(3)$ plus PI (G), FITC-labeled annexin-V (AnnV) plus PI (H), or Hoechst 33324 (I) to determine the $\Delta\psi_m$ loss (G), phosphatidylserine exposure (H), cell death (G-H), or karyorrhexis (I), using either cytofluorometry (G-H) or fluorescence microscopy (I). Image was visualized using a Leica epifluorescent microscope equipped with a 63 ×/1.32-0.6 oil-immersion objective lens and CCD camera (Leica, Heidleberg, Germany). Values are means ± SD (n = 3). (J-K) Immunoblot detection of activated caspase-3 in P39 cells treated with the NF-κB inhibitors BAY11-7082 (J) or bortezomib (K), alone or in combination with z-VAD-fmk. The concentrations of the agents were the same as in panels G-I, and the incubation period was 12 and 24 hours.

Vector Labs, Burlingame, CA). Fluorescent probes were analyzed at × 63 magnification with the epifluorescent microscope DMIRE2 (Leica, Heidelberg, Germany) run by the FW4000 acquisition and analysis software, which allowed background correction (Leica). Two hundred cells were counted per specimen by independent observation.

Statistics

Statistics were analyzed using Excel Software (Microsoft, Redmond, WA), JMP 5.2 software (SAS Institute, Cary, NC), and Scion Image 4.0 (Scion Corporation, Frederick, MD).

Results

Constitutive NF-κB activation in the P39 cell line

The myelomonocytic P39 cell line, which was derived from the bone marrow of an MDS/AML patient,[42] exhibited constitutive NF-κB activation as determined by two different techniques: EMSAs (Figure 1A-B), demonstrating the retention of NF-κB in nuclear DNA (which could be supershifted with a p65-specific antibody; Figure 1B), as well as immunofluorescence staining, revealing the presence of the NF-κB subunit p65 in the nucleus (Figure 1C). Pretreatment of P39 cells with 3 different inhibitors led to the disappearance of NF-κB from nuclei. This applies to an inhibitor of the nuclear transport of NF-κB, the peptide SN50,[43] as well as to small-molecule inhibitors of IKK and BAY11-7082[44] and of the proteasome bortezomib[45] (Figure 1A-D). As expected, bortezomib stimulated the rapid accumulation of phosphorylated IκB in P39 cells (Figure 1E). Moreover, both BAY11-7082 and bortezomib caused the down-regulation of 2 antiapoptotic NF-κB target genes, *Bcl-x_L* and *c-IAP2* (Figure 1F). In this system, BAY11-7082 acted more rapidly than bortezomib (Figure 1F). Altogether these data indicate the presence of a transcriptionally active NF-κB heterodimer in the nucleus of P39 cells. The knock-down of p65 with 2 distinct siRNAs resulted in an increase of spontaneous apoptosis in P39 cells in conditions in which sham transfection, transfection with a scrambled control (Co), or knock-down of emerin expression had no significant prodeath activity (Figure 1G). This indicates that P39 cells require NF-κB activation for survival.

NF-κB inhibition induces caspase-independent cell death in P39 cells

The inhibition of NF-κB using the 2 small-molecule inhibitors BAY11-7082 (Figure 2A-C) and bortezomib (Figure 2D-F) results in the induction of 3 signs of apoptosis, namely a loss of the mitochondrial transmembrane potential ($\Delta\Psi_m$; as determined with the $\Delta\Psi_m$-sensitive dye $DiOC_6(3)$; Figure 2A,D), exposure of phosphatidylserine residues on the outer leaflet of the plasma membrane (as determined by labeling with annexin-V–FITC conjugates; Figure 2B,E), as well as a loss of viability (assessed with the vital dye propidium iodide π; Figure 2C,F). All of these

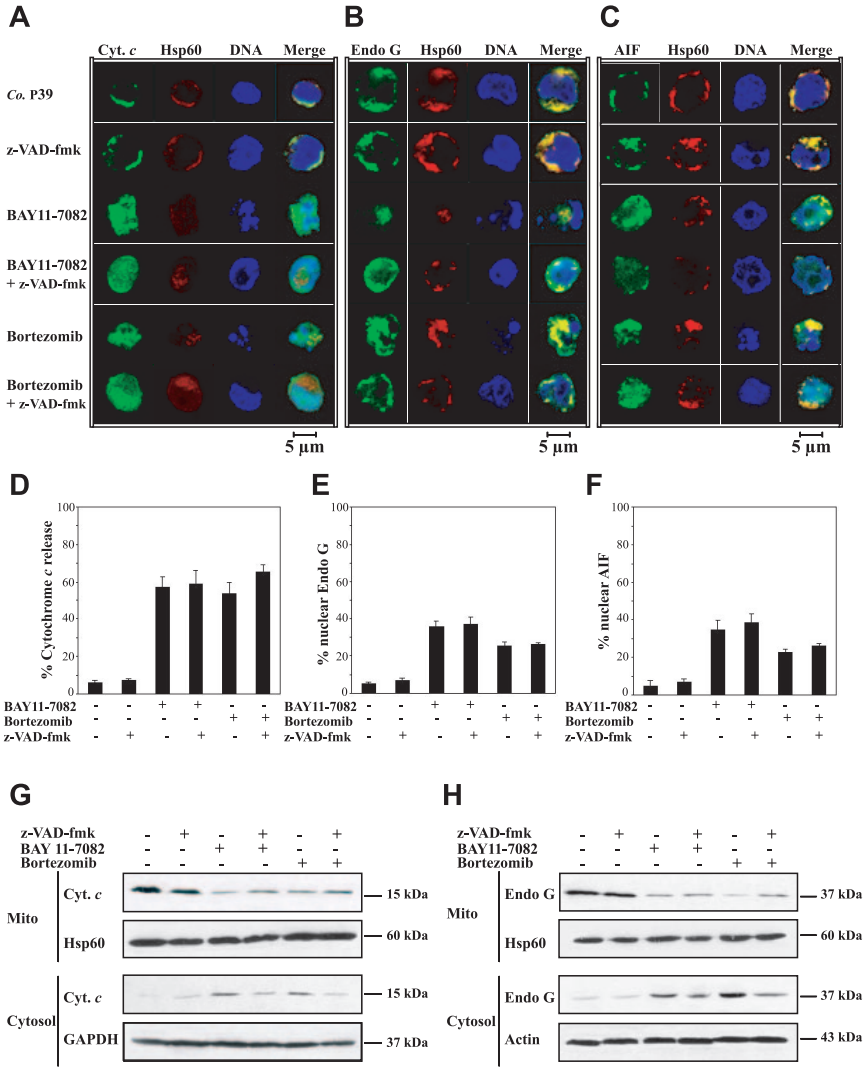

Figure 3. Translocation of caspase-dependent and caspase-independent death effectors from mitochondria of P39 cells treated with NF-κB inhibitors. Cells were treated with standard doses of BAY11-7082, bortezomib, and/or z-VAD-fmk for 12 hours and then stained with the chromatin dye Hoechst 33342 (blue), with an antibody specific for the mitochondrial antigen Hsp60 (red), as well as antibodies specific for Cyt *c* (A,D), EndoG (B,E), or AIF (C,F) (all green). Images were acquired as described for Figure 1C. Representative confocal immunofluorescence pictures are shown (A-C), as well as the percentage of cells demonstrating the mitochondrial release of Cyt *c*, EndoG, or AIF (D-F). Translocation of Cyt *c* and EndoG from mitochondria of P39 cells, as determined by subcellular fractionation and immunoblot (G-H). Cells were treated with BAY11-7082, bortezomib, and/or z-VAD-fmk for 12 hours and then subjected to subcellular fractionation to obtain cytosolic fractions and heavy membrane fractions enriched in mitochondria (mito), followed by immunoblot detection of Cyt *c* (G) or EndoG (H), with GAPDH, actin, or Hsp60 serving as loading controls. This experiment was repeated 3 times yielding similar results.

effects were induced in a concentration- and time-dependent fashion, with BAY11-7082 acting more rapidly than bortezomib. Similar profiles of cell death induction were obtained with SN50 (not shown). The pan-caspase inhibitor z-VAD-fmk failed to protect cells against loss of the $\Delta\Psi_m$ (Figure 2G), phosphatidylserine exposure (Figure 2H), and cell death (Figure 2G-H), although it did prevent bortezomib-induced nuclear fragmentation (karyorrhexis), as assessed by Hoechst 33324 staining and fluorescence microscopy (Figure 2I) as an internal control of its efficacy. Moreover, z-VAD-fmk inhibited the activation of caspase-3 induced by BAY11-7082 or bortezomib (Figure 2J-K). This suggested that NF-κB inhibition induces bona fide apoptosis accompanied by caspase activation, although this caspase activation is not required for cell death. In line with this interpretation, both BAY11-7082 and bortezomib were found to induce the mitochondrial release of cytochrome *c* (Cyt *c*; Figure 3A,D) and that of 2 caspase-independent death effectors, endonuclease G (EndoG; Figure 3B,E) and AIF (Figure 3C,F). This translocation event could be visualized by different techniques, either by subcellular fractionation (Figure 3G-H) or by immunofluorescence, demonstrating that Cyt *c*, EndoG, and AIF lost their colocalization with the mitochondrial marker Hsp60 and exhibited a rather diffuse staining pattern throughout the cell (Figure 3A-C). The release of these proapoptotic factors from mitochondria was not inhibited by z-VAD-fmk (Figure 3), although z-VAD-fmk did attenuate the degree of nuclear chromatin condensation (Figure 3A-C).

ATRA and vitamin D_3 induced myeloid differentiation of P39 cells, leading to the expression of CD11b.[46] CD11b induction was not influenced by z-VAD-fmk (Figure 4A). Neither of these agents inhibits NF-κB (Figure 1A). ATRA (but not vitamin D_3) caused delayed cell death after 72 hours of incubation. This differentiation-induced cell death was inhibited by z-VAD-fmk (Figure 4B-C). At 24 hours, when neither of the differentiating agents induced apoptosis, they partially reduced the proapoptotic effect of BAY11-7082 or bortezomib (Figure 4D-E), although they lost their antiapoptotic effect upon prolonged incubation (Figure 4F-G). Thus, BAY11-7082 or bortezomib can kill both undifferentiated and differentiating P39 cells.

Constitutive NF-κB activation in bone marrow samples from MDS patients

Although cell lines are useful tools to explore the cell biology of hematologic malignancies, they may have acquired nonphysiologic properties. Moreover, it is not clear to which extent the P39 cell line reflects MDS or post-MDS AML. We therefore tested whether bone marrow samples from a series of patients with MDS or MDS patients who progressed to AML (Table 1) would have activated NF-κB, as detectable by EMSA. Patients classified as intermediate 2 or high risk, according to the IPSS criteria, exhibited constitutive NF-κB activation in their bone marrow, whereas this activation was attenuated or undetectable for patients belonging to the low-risk or intermediate 1 groups (Figure 5A). NF-κB activation in high-risk MDS was as intense as in MDS/AML samples (Figure 5A). Immunofluorescence detection of p65, performed on freshly collected bone marrow cells, correlated with the EMSA data (that include a supershift of p65, as detectable in nuclear extracts from purified $CD34^+$ cells from high-risk MDS patients). Purified

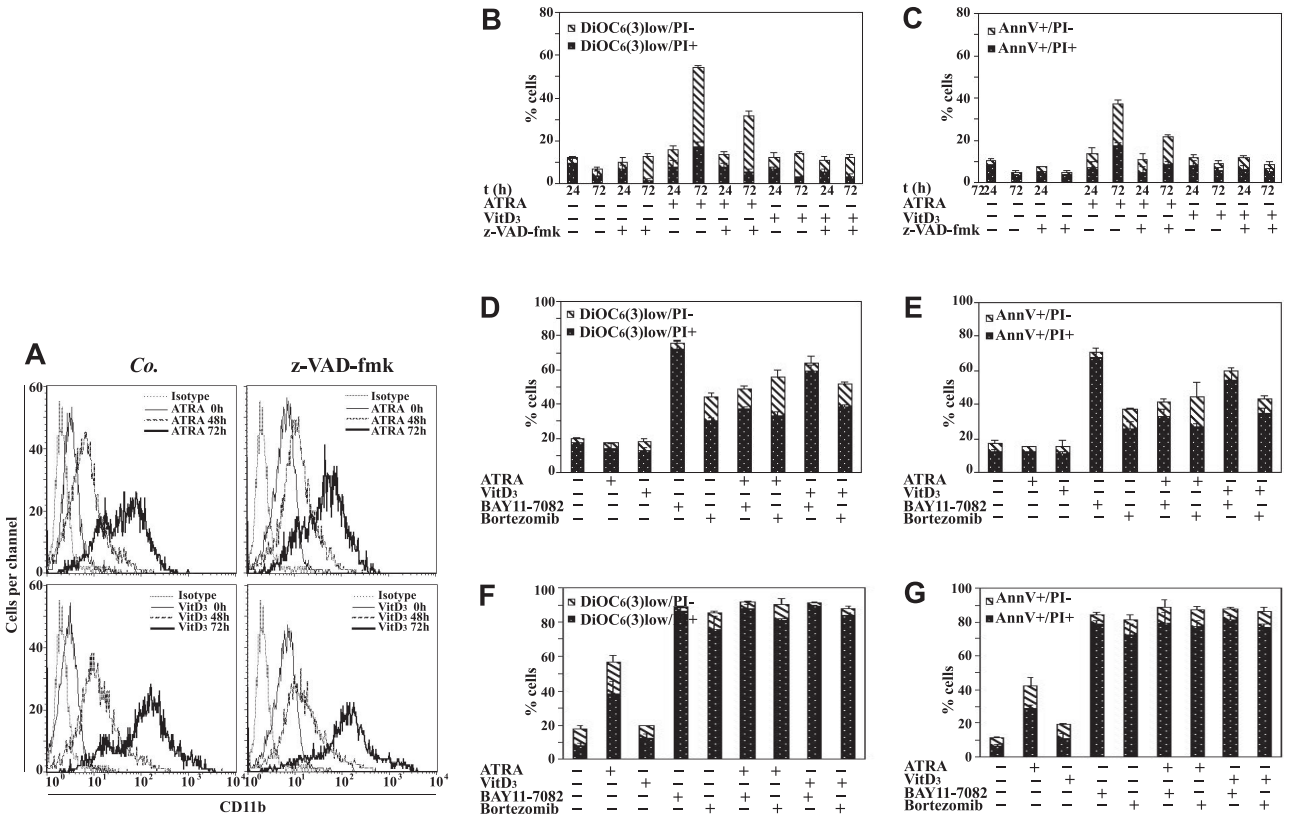

Figure 4. Impact of myeloid differentiation on apoptosis susceptibility. (A) Differentiation of P39 cells. Cells were stimulated for the indicated period with ATRA or vitamin D_3 in the absence or presence of z-VAD-fmk, followed by immunocytofluorometric detection of the differentiation marker CD11b. (B-C) Differentiation-associated cell death. Cells treated as in panel A were analyzed for any of 3 apoptotic parameters, namely $\Delta\psi_m$ loss (B), phosphatidyl serine (PS) exposure (C), and PI staining (B-C). (D-G) Effect of NF-κB inhibitors on differentiating P39 cells. Cells were cultured with the indicated combinations of ATRA, vitamin D_3, BAY11-7082, and/or bortezomib for 24 hours (D-E) or 72 hours (F-G), then labeled with $DiOC_6(3)$ plus PI (D,F) or FITC-labeled annexin-V plus PI (E,G), and subjected to flow cytometric analyses. This experiment was repeated 4 times, yielding comparable results. Values are expressed as means ± SD; n = 3.

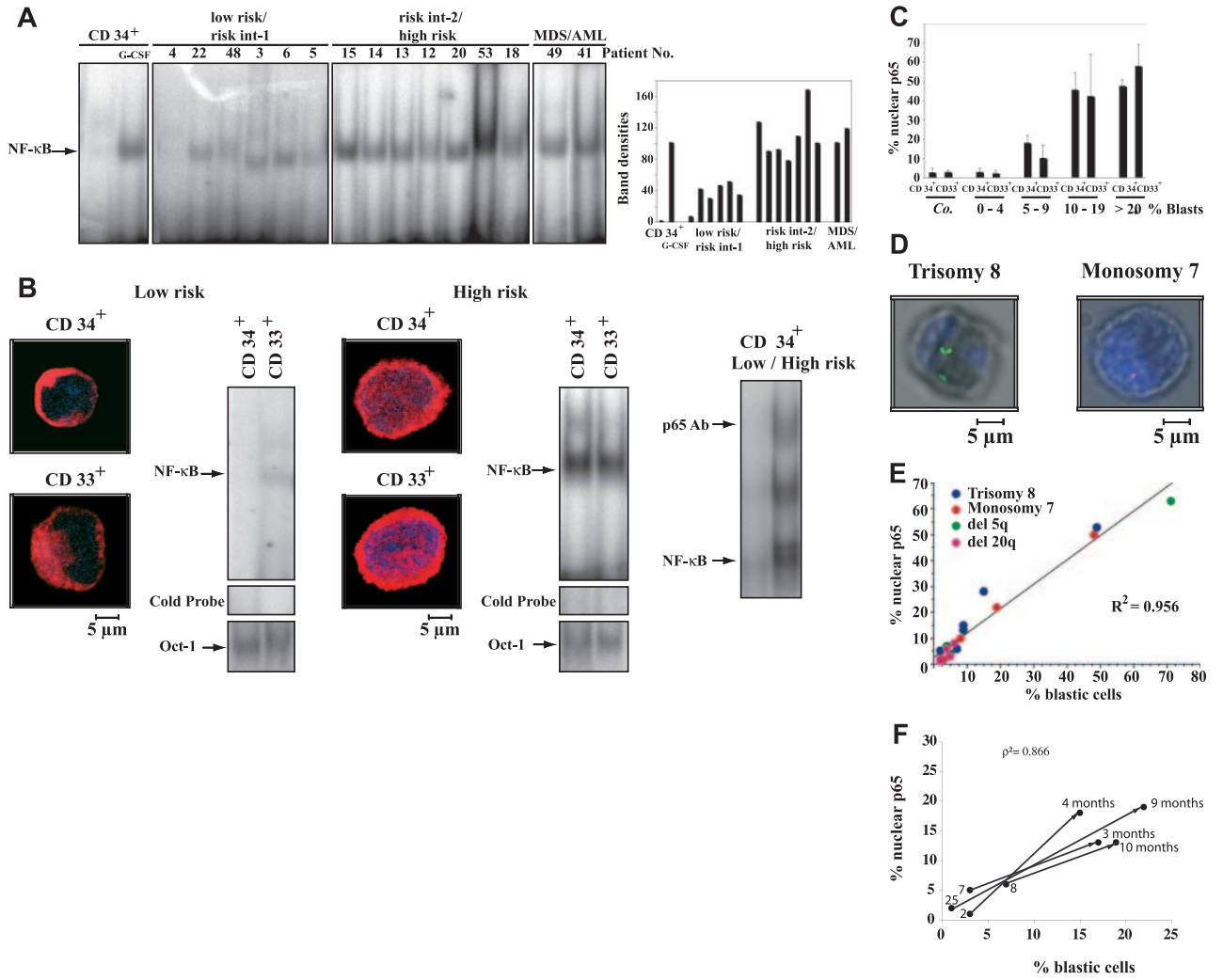

Figure 5. NF-κB activation in bone marrow samples from MDS patients. (A) Evidence for NF-κB activation in high-risk MDS, as determined by EMSA performed on total bone marrow samples. Bone marrow aspirates from the indicated low- or high-risk patients (same numbers as in Table 1) were analyzed by EMSA, as described in "Patients, materials, and methods." Cord blood CD34$^+$ cells before and after stimulation with G-CSF served as negative and positive control, respectively. The intensity of bands was quantified (right panel). (B) Evidence of NF-κB activation in purified CD34$^+$ or CD33$^+$ cells from high-risk MDS bone marrow samples. Cells from patients 24 and 54 (Table 1), representing low- and high-risk MDS, respectively, were subjected to confocal immunofluorescence determination of p65 activation and EMSA detection of NF-κB alone or with the p65 antibody (supershift in right panel), as well as Oct-1 as a loading control. Images were acquired as described for Figure 1C. (C) Percentage of purified CD34$^+$ or CD33$^+$ cells with nuclear p65 staining among different MDS patient groups classified according to the percentage of bone marrow blast infiltration. Samples from 3 different control individuals, as well as different patients (nos. 1, 24, 34, 35, and 37 representing MDS patients with <5% blast; nos. 9, 11, 27, 28, 38, and 47 for patients with 5%-9% blasts; nos. 16, 17, 20, 54, and 57 for patients with >10% blasts; nos. 21 and 32 for >20% blasts), were subjected to p65 staining as in panel B, and the frequency of cells exhibiting nuclear p65 staining was determined. Values are expressed as means ± SD; n = 3. (D) Combined detection of nuclear p65 and cytogenetic alterations. Bone marrow aspirates from untreated MDS patients were subjected to the simultaneous immunohistochemical detection of p65 and FISH, using probes specific for the centromeres of chromosomes 7 and 8. Note that cells with manifest cytogenetic alterations (trisomy 8 in left panel or monosomy 7 in right panel) can exhibit the presence of p65 (gray) in the nucleus whereas euploid cells have p65 in the cytoplasm (not shown). Fluorescence micrographs were acquired as described for Figure 2I. (E) Correlation between blast counts and the frequency of cells with nuclear p65 (same patients as in Table 2 and patients 36, 39, and 42-46). The coefficient of correlation was calculated using linear regression. (F) Longitudinal study of blast counts and nuclear p65 in MDS patients. Bone marrow aspirates from patients 2, 7, 8, and 25 obtained at the beginning of clinical monitoring (values in Table 1) or several months later (as indicated in the figure) were subjected to immunofluorescence analyses, showing an increase in p65 translocation to the nucleus. Blast counts and p65 translocation were correlated using the Spearman correlation model.

CD34$^+$ or CD33$^+$ cells from high-risk (but not from low-risk) MDS patients exhibited the nuclear translocation of p65 as well as EMSA-detectable NF-κB. This is shown for representative patients in Figure 5B and quantified for a cohort of 18 patients in Figure 5C. We found that there was a positive correlation between the percentage of blasts in MDS bone marrow samples and the frequency of CD34$^+$ or CD33$^+$ cells with nuclear p65 (Figure 5C). To address the question whether NF-κB activation would be restricted to the mutated cancer stem population and its derivatives or whether it would also affect nonmutated, normal cells in the bone marrow, we combined the immunohistochemical detection of p65 with the detection of chromosomal aberrations by FISH at the single-cell level. Using this technique, we found that cells with nuclear p65 possessed cytogenetic alterations when patients with trisomy 8 or monosomy 7 were analyzed (Figure 5D). While all cells with p65 translocation demonstrated MDS-associated cytogenetic aberrations, there was a fraction of cells with trisomy 8 or monosomy 7 that had no p65 in the nucleus. Indeed, the number of bone marrow cells with activated NF-κB correlated ($P < .001$) with the percentage of blasts found in the bone marrow. This finding was obtained for the patients with trisomy 8 or monosomy 7 (Table 2), as well as for the 5q$^-$ and 20q$^-$ MDS patients investigated (Figure 5E). The correlation between blast counts and nuclear p65 translocation was observed irrespective of the underlying cytogenetic alteration or the degree of cytopenias (Tables 1-2). Importantly, we found that p65 translocation to the nucleus correlated with disease progression in a longitudinal study performed on 4 patients (Figure 5F). Altogether, these findings

Table 2. Nuclear translocation of p65 in BM cells of MDS patients

Patient no.	BM blasts, %	Karyotype	KA+ cells, %		KA− cells, %	
			$p65^{Nuc}$	$p65^{Cyt}$	$p65^{Nuc}$	$p65^{Cyt}$
23	2	47, XY, +8	5	28	< 1	67
26	4	47, XY, +8	6	38	< 1	56
28	7	47, XX, +8	6	23	< 1	71
29	9	47, XY, +8	13	50	< 1	37
30	9	47, XY, +8	14	33	< 1	53
31	15	47, XX, +8	23	47	< 1	30
33	49	47, XX, +8	53	16	< 1	31
50	2	45, XY, −7	2	44	< 1	54
51	3	45, XX, −7	2	49	< 1	49
52	8	45, XY, −7	10	26	< 1	64
54	19	45, XX, −7	22	28	< 1	50
55	48	45, XX, −7	49	10	< 1	41

KA indicates karyotype abnormal; Nuc, nuclear; and Cyt, cytosolic.

indicate a strong constitutive NF-κB activation restricted to the blast population carrying cytogenetic aberrations.

NF-κB inhibition triggers the mitochondrial death pathway in MDS cells

If NF-κB acts as an antiapoptotic factor in MDS, its inhibition should precipitate the cell death of MDS blasts ex vivo. BAY11-7082 or bortezomib abolished NF-κB activation when added to bone marrow samples from high-risk MDS patients (Figure 6A). Simultaneously, BAY11-7082– or bortezomib-treated cells manifested the mitochondrial release of Cyt *c*, EndoG, and AIF, correlating with chromatin condensation as determined by immunofluorescence in both $CD34^+$ (Figure 6B) and $CD33^+$ (Figure 6C) cells. Cytofluorometric analyses confirmed that BAY11-7082 and bortezomib enhanced cell death when added to bone marrow samples from high-risk MDS patients (Figure 7A,C). However, neither of the 2 NF-κB inhibitors did enhance the elevated spontaneous apoptosis affecting low-risk MDS samples (Figure 7A,C), in accord with the fact that low-risk MDS patients exhibit a low level of NF-κB activation, correlating with highly spontaneous apoptosis (Figure 7B). Altogether, these data indicate that NF-κB inhibition can trigger the death of MDS blasts through a mitochondrial pathway involving the release of caspase activators and caspase-independent death effectors.

Discussion

The data contained in this article indicate that NF-κB is activated within blasts found in MDS bone marrow samples. The strong correlation between blast counts and p65 translocation (Figure 5E) suggests that this latter parameter can be used as a surrogate marker of disease progression. In line with this hypothesis, high-risk MDS exhibits a higher frequency of cells with nuclear p65 (Figure 5B-C) and more intense bands reflecting NF-κB activation in EMSA (Figure 5A-B) compared with low-risk MDS. Thus, high-risk MDS behaves like post-MDS AML (Figure 5A,C) with regard to a strong constitutive NF-κB activation. These data differ from 2 previous reports in which, among a limited cohort of MDS patients (total no. 11), no evidence for NF-κB activation[32] and no correlation with the FAB MDS classification[33] was found in MDS bone marrow samples. In those reports, however, no attempts were undertaken to purify $CD34^+$ or $CD33^+$ from the bone marrow or to correlate NF-κB activation with blast counts. In contrast, our data confirm a

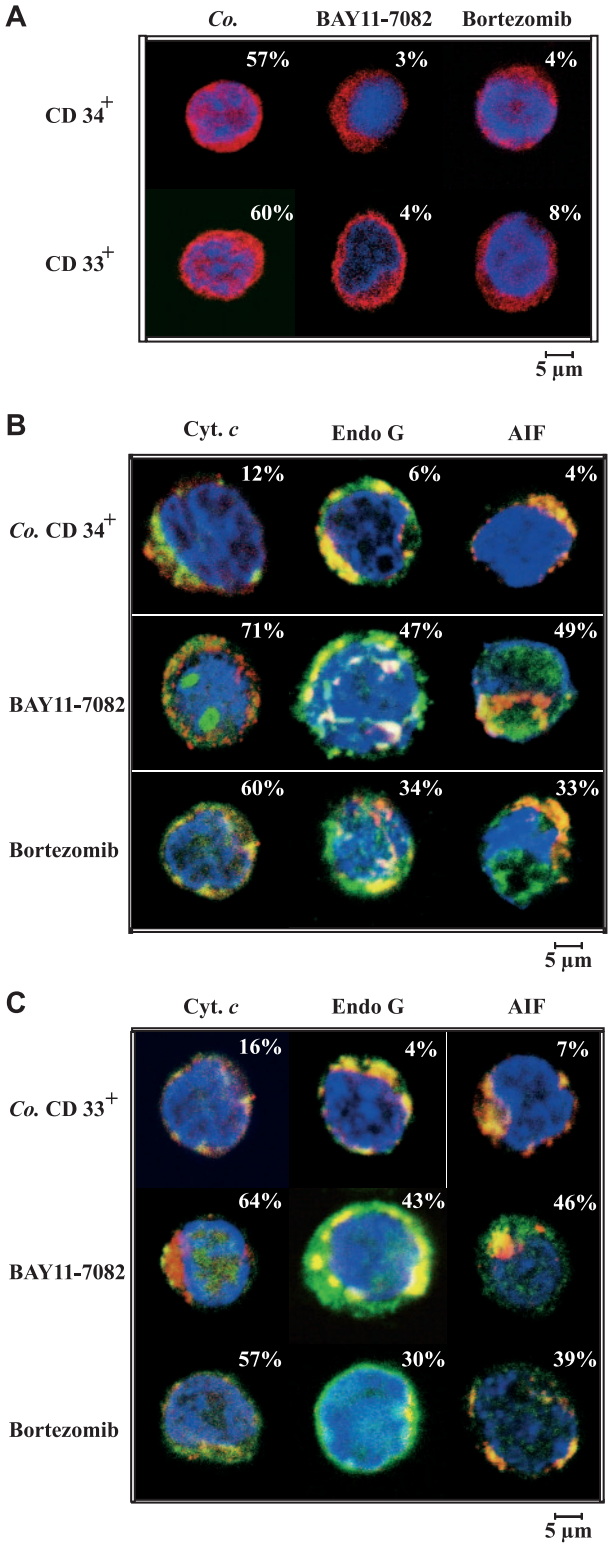

Figure 6. Inhibition of NF-κB activation in MDS bone marrow samples with BAY11-7082 or bortezomib. (A) Immunofluorescence detection of p65. Bone marrow samples from a high-risk MDS patient (Table 1 no. 54) were precultured for 6 hours in the absence or presence of BAY11-7082 or bortezomib and then subjected to confocal immunofluorescence analyses. Percentages refer to the fraction of cells exhibiting nuclear p65 staining. Similar results were obtained for samples from 2 other high-risk MDS patients (Table 1 nos. 19 and 57). (B-C) BAY11-7082 or bortezomib induced translocation of mitochondrial death effectors in bone marrow cells from high-risk MDS patients. Bone marrow aspirates from the same patients as in panel A were purified to yield $CD34^+$ (B) or $CD33^+$ (C) cells and cultured ex vivo, in the presence or absence of BAY11-7082 or bortezomib, and then stained with antibodies specific for Hsp60 (red), Cyt *c*, EndoG, and AIF (all green). Representative cells are shown. Percentage values refer to the cells exhibiting mitochondrial release of Cyt *c*, EndoG, or AIF in the indicated conditions. Images were acquired as described for Figure 1C.

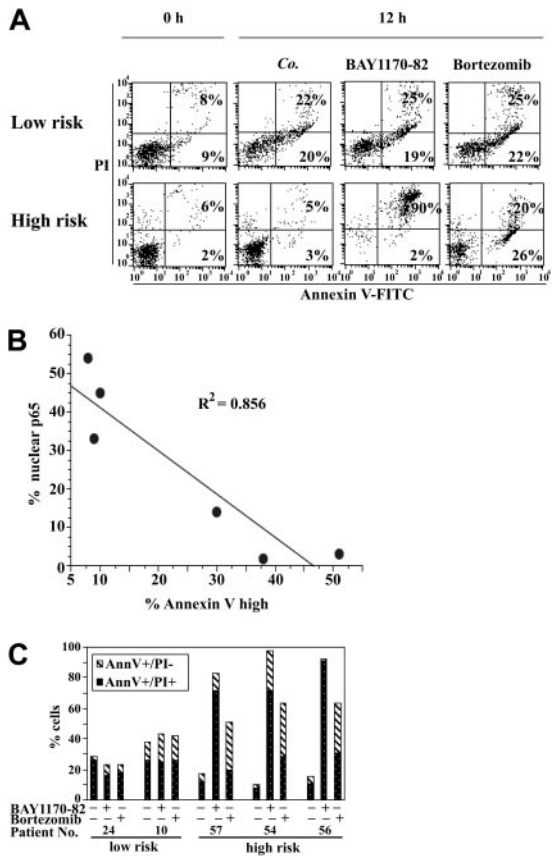

Figure 7. Ex vivo killing of bone marrow cells from MDS patients by BAY11-7082 or bortezomib. Representative fluorescence-activated cell sorter (FACS) pictograms as obtained for $CD34^+$ cells from patients 24 with low-risk MDS and 54 with high-risk MDS (A) (Table 1) 12 hours after culture in the presence or absence of BAY11-7082 or bortezomib. The numbers in each quadrant indicate the percentage of cells exhibiting the indicated changes. (B) Inverse correlation between p65 translocation and spontaneous apoptosis upon overnight in vitro culture of $CD34^+$ cells from different MDS patients. Each point represents 1 patient. The correlation coefficient was determined by linear regression. (C) Statistical comparison of low- and high-risk patients treated and evaluated as in panel A. Note that BAY11-7082 or bortezomib only enhanced the rate of spontaneous apoptosis in high-risk but not in low-risk MDS.

recent study (total no. of patients 25) suggesting a positive correlation between high-risk MDS and NF-κB activation.[34]

The molecular etiology of NF-κB activation in high-risk MDS remains elusive. As demonstrated by combined immunohistochemical p65 detection and FISH, NF-κB activation is restricted to cells bearing cytogenetic alterations, at least in the case of trisomy 8 and monosomy 7 investigated in this study (Figure 5D). TNF and TRAIL are potent NF-κB inducers[47,48] and are reportedly upregulated in MDS bone marrows[49,50] and coresponsible for NF-κB activation.[34] However, it is unlikely that these diffusible agents account for NF-κB activation in MDS because they would also activate NF-κB in a fraction of normal cells—that is, cells without cytogenetic alterations. CD95/Fas, which can signal NF-κB activation upon interaction with CD95L/FasL,[51,52] is activated in trisomy 8 but not in monosomy 7,[53] suggesting (but by no means excluding) that death receptors are not responsible for NF-κB activation in MDS blasts. Rather, it would appear plausible that the NF-κB activation occurring in MDS blasts results in a cell-autonomous fashion, perhaps as an indirect result of secondary mutations that determine neoplastic transformation. Indeed, in several MDS patients without cytogenetic alterations detectable by conventional karyotyping, a fraction of cells exhibited NF-κB activation (Table 1 and Figure 5A,C; patients 11-21), and NF-κB activation appeared to be a function of blast counts, irrespective of the underlying cytogenetic alteration.

NF-κB activates multiple target genes,[54] an important fraction of which exerts antiapoptotic and proliferative functions. Low-risk MDS, in which NF-κB is not activated, is characterized by an enhanced apoptotic turnover of differentiating bone marrow cells.[55,56] In contrast, high-risk MDS with low intramedullar apoptosis[57,58] demonstrates NF-κB activation. It is tempting to speculate that the inverse correlation between apoptosis and NF-κB activation could reflect (one of) the mechanism(s) through which apoptosis is suppressed in high-risk MDS. In favor of this interpretation, we found that suppression of NF-κB by an IKK inhibitor or by a proteasome inhibitor enhanced apoptosis in high-risk MDS bone marrow cells ex vivo, yet had no such effect on low-risk MDS (Figures 6-7). Thus, high-risk MDS blasts isolated ex vivo responded to BAY-7082 and bortezomib by apoptosis (Figures 6-7) in a similar fashion as the P39 cell line, which was isolated from the blood of a high-risk MDS patient.[42] Both freshly isolated MDS blasts and P39 cells succumbed to NF-κB inhibition without the need of additional cytotoxic stimuli. Both inhibited constitutive NF-κB activation with p65 translocation to the nucleus (Figures 1B-D and 6A), which is not curtailed by differentiation induced in vitro (Figures 1A and 4) or in vivo (Figure 5B) to CD11b-expressing or CD33-expressing myeloid cells, respectively. Moreover, this constitutive NF-κB activation was fully blocked by BAY11-7082 or bortezomib in patient-derived MDS blasts (Figure 6A) and in the P39 cell line (Figure 1A-D). Both primary MDS cells and P39 cells manifested mitochondrial changes culminating in the release of cytochrome *c*, AIF, and endonuclease G (Figures 3 and 6), as well as bone fide apoptosis with nuclear pyknosis and karyorrhexis (Figures 2I and 6), when NF-κB was inhibited. Although caspase inhibition could prevent advanced chromatin condensation (Figure 2I), it had no or little effect on the irreversible loss of vital cellular functions (Figure 2), in accord with the fact that caspase inhibition also failed to suppress the mitochondrial release of the 2 caspase-independent death effectors AIF and EndoG (Figure 3).

Altogether, these data suggest that NF-κB is vital for MDS blasts and that NF-κB inhibition might constitute a strategy for the eradication of such cells. Thus bortezomib or alternative, more-specific NF-κB inhibitors that are being developed might be tested alone or in combination with other agents for the treatment of MDS.

Acknowledgments

We thank Bertrand Billemont and Antoine Tesnière (Institut Gustave Roussy, Villejuif, France) for statistics; Jalil Abdelali (Institut Gustave Roussy, Villejuif, France) for confocal microscopy; Karen Brumpt (Hôpital Beaujon, Clichy, France), Alain Chapel (Hôpital St Antoine, Paris, France), and Annelise Benanceur-Griscelli (IGR, Villejuif, France) for patient samples; and Marie Pequignot for support in immunohistochemistry.

References

1. Fenaux P. Myelodysplastic syndromes: from pathogenesis and prognosis to treatment. Semin Hematol. 2004;41:6-12.
2. Vardiman JW, Harris NL, Brunning RD. The World Health Organization (WHO) classification of the myeloid neoplasms. Blood. 2002;100:2292-2302.
3. Greenberg P, Cox C, LeBeau MM, et al. International scoring system for evaluating prognosis in myelodysplastic syndromes. Blood. 1997;89:2079-2088.

4. Padua RA, West RR. Oncogene mutation and prognosis in the myelodysplastic syndromes. Br J Haematol. 2000;111:873-874.
5. Shih LY, Huang CF, Wang PN, et al. Acquisition of FLT3 or N-ras mutations is frequently associated with progression of myelodysplastic syndrome to acute myeloid leukemia. Leukemia. 2004;18:466-475.
6. Quesnel B, Guillerm G, Vereecque R, et al. Methylation of the p15(INK4b) gene in myelodysplastic syndromes is frequent and acquired during disease progression. Blood. 1998;91:2985-2990.
7. Fenaux P. Chromosome and molecular abnormalities in myelodysplastic syndromes. Int J Hematol. 2001;73:429-437.
8. Shetty V, Hussaini S, Broady-Robinson L, et al. Intramedullary apoptosis of hematopoietic cells in myelodysplastic syndrome patients can be massive: apoptotic cells recovered from high-density fraction of bone marrow aspirates. Blood. 2000;96:1388-1392.
9. Parker JE, Mufti GJ. Ineffective haemopoiesis and apoptosis in myelodysplastic syndromes. Br J Haematol. 1998;101:220-230.
10. Parker JE, Mufti GJ, Rasool F, Mijovic A, Devereux S, Pagliuca A. The role of apoptosis, proliferation, and the Bcl-2-related proteins in the myelodysplastic syndromes and acute myeloid leukemia secondary to MDS. Blood. 2000;96:3932-3938.
11. Tehranchi R, Fadeel B, Forsblom AM, et al. Granulocyte colony-stimulating factor inhibits spontaneous cytochrome c release and mitochondria-dependent apoptosis of myelodysplastic syndrome hematopoietic progenitors. Blood. 2003;101:1080-1086.
12. Boudard D, Sordet O, Vasselon C, et al. Expression and activity of caspases 1 and 3 in myelodysplastic syndromes. Leukemia. 2000;14:2045-2051.
13. Merchant SH, Gonchoroff NJ, Hutchison RE. Apoptotic index by Annexin V flow cytometry: adjunct to morphologic and cytogenetic diagnosis of myelodysplastic syndromes. Cytometry. 2001;46:28-32.
14. Sloand EM, Mainwaring L, Fuhrer M, et al. Preferential suppression of trisomy 8 versus normal hematopoietic cell growth by autologous lymphocytes in patients with trisomy 8 myelodysplastic syndrome. Blood. 2005;106:841-851.
15. Claessens YE, Bouscary D, Dupont JM, et al. In vitro proliferation and differentiation of erythroid progenitors from patients with myelodysplastic syndromes: evidence for Fas-dependent apoptosis. Blood. 2002;99:1594-1601.
16. Stasi R, Amadori S. Infliximab chimaeric anti-tumour necrosis factor alpha monoclonal antibody treatment for patients with myelodysplastic syndromes. Br J Haematol. 2002;116:334-337.
17. Zang DY, Goodwin RG, Loken MR, Bryant E, Deeg HJ. Expression of tumor necrosis factor-related apoptosis-inducing ligand, Apo2L, and its receptors in myelodysplastic syndrome: effects on in vitro hemopoiesis. Blood. 2001;98:3058-3065.
18. Boudard D, Vasselon C, Bertheas MF, et al. Expression and prognostic significance of Bcl-2 family proteins in myelodysplastic syndromes. Am J Hematol. 2002;70:115-125.
19. Takada Y, Andreeff M, Aggarwal BB. Indole-3-carbinol suppresses NF-{kappa}B and I{kappa} B{alpha} kinase activation causing inhibition of expression of NF-{kappa}B-regulated antiapoptotic and metastatic gene products and enhancement of apoptosis in myeloid and leukemia cells. Blood. 2005;106:641-649.
20. Aggarwal BB. Nuclear factor-kappaB: the enemy within. Cancer Cell. 2004;6:203-208.
21. Turco MC, Romano MF, Petrella A, Bisogni R, Tassone P, Venuta S. NF-kappaB/Rel-mediated regulation of apoptosis in hematologic malignancies and normal hematopoietic progenitors. Leukemia. 2004;18:11-17.
22. Bharti AC, Shishodia S, Reuben JM, et al. Nuclear factor-kappaB and STAT3 are constitutively active in CD138+ cells derived from multiple myeloma patients, and suppression of these transcription factors leads to apoptosis. Blood. 2004;103:3175-3184.
23. Cerimele F, Battle T, Lynch R, et al. Reactive oxygen signaling and MAPK activation distinguish Epstein-Barr Virus (EBV)-positive versus EBV-negative Burkitt's lymphoma. Proc Natl Acad Sci U S A. 2005;102:175-179.
24. Sinha-Datta U, Horikawa I, Michishita E, et al. Transcriptional activation of hTERT through the NF-kappaB pathway in HTLV-I-transformed cells. Blood. 2004;104:2523-2531.
25. Guzman ML, Neering SJ, Upchurch D, et al. Nuclear factor-kappaB is constitutively activated in primitive human acute myelogenous leukemia cells. Blood. 2001;98:2301-2307.
26. Israel A. Signal transduction: a regulator branches out. Nature. 2003;423:596-597.
27. Hatakeyama S, Kitagawa M, Nakayama K, et al. Ubiquitin-dependent degradation of IkappaBalpha is mediated by a ubiquitin ligase Skp1/Cul 1/F-box protein FWD1. Proc Natl Acad Sci U S A. 1999;96:3859-3863.
28. Grumont RJ, Strasser A, Gerondakis S. B cell growth is controlled by phosphatidylinosotol 3-kinase-dependent induction of Rel/NF-kappaB regulated c-myc transcription. Mol Cell. 2002;10:1283-1294.
29. Lam LT, Davis RE, Pierce J, et al. Small molecule inhibitors of IkappaB kinase are selectively toxic for subgroups of diffuse large B-cell lymphoma defined by gene expression profiling. Clin Cancer Res. 2005;11:28-40.
30. Richardson PG, Barlogie B, Berenson J, et al. A phase 2 study of bortezomib in relapsed, refractory myeloma. N Engl J Med. 2003;348:2609-2617.
31. Orlowski RZ, Voorhees PM, Garcia RA, et al. Phase 1 trial of the proteasome inhibitor bortezomib and pegylated liposomal doxorubicin in patients with advanced hematologic malignancies. Blood. 2005;105:3058-3065.
32. Bueso-Ramos CE, Rocha FC, Shishodia S, et al. Expression of constitutively active nuclear-kappa B RelA transcription factor in blasts of acute myeloid leukemia. Hum Pathol. 2004;35:246-253.
33. Sanz C, Richard C, Prosper F, Fernandez-Luna JL. Nuclear factor k B is activated in myelodysplastic bone marrow cells. Haematologica. 2002;87:1005-1006.
34. Kerbauy DM, Lesnikov V, Abbasi N, Seal S, Scott B, Deeg HJ. NF-{kappa}B and FLIP in arsenic trioxide (ATO)-induced apoptosis in myelodysplastic syndromes (MDS). Blood. Prepublished on August 16, 2005, as DOI 10.1182/blood-2005-04-1424.
35. Hassan Z, Fadeel B, Zhivotovsky B, Hellstrom-Lindberg E. Two pathways of apoptosis induced with all-trans retinoic acid and etoposide in the myeloid cell line P39. Exp Hematol. 1999;27:1322-1329.
36. Harborth J, Elbashir SM, Bechert K, Tuschl T, Weber K. Identification of essential genes in cultured mammalian cells using small interfering RNAs. J Cell Science. 2001;114:4557-4565.
37. Zamzami N, Kroemer G. Methods to measure membrane potential and permeability transition in the mitochondria during apoptosis. Methods Mol Biol. 2004;282:103-115.
38. Castedo M, Ferri K, Roumier T, Metivier D, Zamzami N, Kroemer G. Quantitation of mitochondrial alterations associated with apoptosis. J Immunol Methods. 2002;265:39-47.
39. Castedo M, Hirsch T, Susin SA, et al. Sequential acquisition of mitochondrial and plasma membrane alterations during early lymphocyte apoptosis. J Immunol. 1996;157:512-521.
40. Zamzami N, Marchetti P, Castedo M, et al. Sequential reduction of mitochondrial transmembrane potential and generation of reactive oxygen species in early programmed cell death. J Exp Med. 1995;182:367-377.
41. Carvalho G, Lefaucheur C, Cherbonnier C, et al. Chemosensitization by erythropoietin through inhibition of the NF-kappaB rescue pathway. Oncogene. 2005;24:737-745.
42. Nagai M, Seki S, Kitahara T, et al. A novel human myelomonocytoid cell line, P39/Tsugane, derived from overt leukemia following myelodysplastic syndrome. Gann. 1984;75:1100-1107.
43. Lin YZ, Yao SY, Veach RA, Torgerson TR, Hawiger J. Inhibition of nuclear translocation of transcription factor NF-kappa B by a synthetic peptide containing a cell membrane-permeable motif and nuclear localization sequence. J Biol Chem. 1995;270:14255-14258.
44. Engedal N, Blomhoff HK. Combined action of ERK and NF kappa B mediates the protective effect of phorbol ester on Fas-induced apoptosis in Jurkat cells. J Biol Chem. 2003;278:10934-10941.
45. Adams J. The proteasome: a suitable antineoplastic target. Nat Rev Cancer. 2004;4:349-360.
46. Anzai N, Kawabata H, Hirama T, et al. Marked apoptosis of human myelomonocytic leukemia cell line P39: significance of cellular differentiation. Leukemia. 1994;8:446-453.
47. Wachter T, Sprick M, Hausmann D, et al. cFLIPL inhibits tumor necrosis factor-related apoptosis-inducing ligand-mediated NF-kappaB activation at the death-inducing signaling complex in human keratinocytes. J Biol Chem. 2004;279:52824-52834.
48. Van Antwerp DJ, Martin SJ, Kafri T, Green DR, Verma IM. Suppression of TNF-alpha-induced apoptosis by NF-kappaB. Science. 1996;274:787-789.
49. Campioni D, Secchiero P, Corallini F, et al. Evidence for a role of TNF-related apoptosis-inducing ligand (TRAIL) in the anemia of myelodysplastic syndromes. Am J Pathol. 2005;166:557-563.
50. Benesch M, Platzbecker U, Ward J, Deeg HJ, Leisenring W. Expression of FLIP(Long) and FLIP(Short) in bone marrow mononuclear and CD34+ cells in patients with myelodysplastic syndrome: correlation with apoptosis. Leukemia. 2003;17:2460-2466.
51. Teixeiro E, Daniels MA, Hausmann B, et al. T cell division and death are segregated by mutation of TCRbeta chain constant domains. Immunity. 2004;21:515-526.
52. Ponton A, Clement MV, Stamenkovic I. The CD95 (APO-1/Fas) receptor activates NF-kappaB independently of its cytotoxic function. J Biol Chem. 1996;271:8991-8995.
53. Sloand EM, Kim S, Fuhrer M, et al. Fas-mediated apoptosis is important in regulating cell replication and death in trisomy 8 hematopoietic cells but not in cells with other cytogenetic abnormalities. Blood. 2002;100:4427-4432.
54. Karin M, Lin A. NF-kappaB at the crossroads of life and death. Nat Immunol. 2002;3:221-227.
55. Novitzky N, Mohamed R, Finlayson J, du Toit C. Increased apoptosis of bone marrow cells and preserved proliferative capacity of selected progenitors predict for clinical response to anti-inflammatory therapy in myelodysplastic syndromes. Exp Hematol. 2000;28:941-949.
56. Parker J, Mufti GJ. Ras and myelodysplasia: lessons from the last decade. Semin Hematol. 1996; 33:206-224.
57. Suarez L, Vidriales MB, Garcia-Larana J, et al. CD34+ cells from acute myeloid leukemia, myelodysplastic syndromes, and normal bone marrow display different apoptosis and drug resistance-associated phenotypes. Clin Cancer Res. 2004;10:7599-7606.
58. van de Loosdrecht AA, Brada SJ, Blom NR, et al. Mitochondrial disruption and limited apoptosis of erythroblasts are associated with high risk myelodysplasia: an ultrastructural analysis. Leuk Res. 2001;25:385-393.